

# Synthesis, Structure, and Bonding of the Novel Cluster Compound KTI with Isolated $Tl_6^{6-}$ Ions

Zhenchao Dong and John D. Corbett\*

Contribution from Ames Laboratory—DOE<sup>1</sup> and Department of Chemistry, Iowa State University, Ames, Iowa 50011

Received August 9, 1993<sup>⊙</sup>

**Abstract:** The unprecedented naked cluster  $Tl_6^{6-}$  occurs in the incongruently melting line compound KTI (*Cmca*,  $Z = 24$ ,  $a = 15.239(4)$  Å,  $b = 15.069(4)$  Å,  $c = 8.137(2)$  Å;  $R/R_w = 3.7\%/3.9\%$  for 462 independent reflections and 33 variables). The  $C_{2h}$  anion consists of a thallium octahedron tetragonally compressed to produce shorter axial–waist distances (3.06–3.08 Å), an enlarged rectangular waist (3.34–3.47 Å), and a 1.0-Å difference in trans distances. Potassium atoms bridge between clusters and show somewhat specific orientations on cluster vertices, edges, and faces. The compound is diamagnetic. The hypoelectronic cluster structure with  $2n$  6p electrons in skeletal orbitals derives from the observed compression, in analogy to recent results for two indium clusters. Extended Hückel calculations show the expected splitting of the p-orbital-based  $t_{1u}$  on compression of octahedral  $Tl_6$  to elevate the  $a_{2u}$  component, although the available orbital parameter sets are not completely satisfactory. Relationships with some corresponding liquid alloy systems are noted.

## Introduction

Octahedral  $M_6$  units are typical frameworks within the transition-metal and rare-earth-metal cluster halides, chalcogenides, etc.<sup>2,3</sup> Among the main-group elements, all examples of octahedra are also exo-bonded— $B_6H_6^{2-}$ ,  $C_2B_4H_6^{4-}$ , the octahedra linked at all vertices in the hexaborides of Na, K, Ca, and La<sup>5</sup> or in layers in  $A_2In_3$  ( $A = Rb, Cs$ ),<sup>6</sup> and the ligated  $Sn_6(Cr(CO)_3)_6^{2-}$ .<sup>7</sup> In all of these cases, 14 electrons are involved in skeletal (p orbital) bonding, consistent with Wade's  $2n + 2$  rule. Other sized polyhedra of main-group elements with classical electronic structures are well-known in "naked" Zintl ions, e.g.,  $Sn_9^{4-}$ ,  $Pb_5^{2-}$ ,  $Sn_2Bi_2^{2-}$ , and  $Sb_7^{3-}$ .<sup>8</sup> Among the electron-poorer elements, boron in general forms a large number of isolated binary (or higher) clusters,<sup>9</sup> but compounds with discrete clusters become very rare for Al, Ga, and In, amounting to mainly  $(Al-iBu)_{12}^{2-}$ <sup>10</sup> and the recently reported  $In_{11}^{7-}$ <sup>11</sup> and  $In_4^{8-}$ .<sup>12</sup> Therefore, it is rather surprising that thallium comes back to be so rich in discrete cluster chemistry. Two examples are analogous to indium chemistry, the classical tetrahedral  $Tl_4^{8-}$  in  $Na_2Tl^{13}$  and the pentacapped trigonal prismatic  $Tl_{11}^{7-}$  in  $A_8Tl_{11}$  ( $A = K, Rb, Cs$ ).<sup>14,15</sup> In this article, we report the unprecedented "naked"

and hypoelectronic cluster  $Tl_6^{6-}$  that occurs in KTI in the form of tetragonally compressed octahedra. This composition was first reported by Zintl and Brauer, who established only that the phase was not isostructural with either the classic NaTI (stuffed diamond) or  $\beta$ -brass.<sup>16</sup> Details on the isolated  $Tl_5^{7-}$  and  $Tl_9^{9-}$  cluster anions that occur in  $Na_2K_2Tl_{19}$  will also be described shortly.<sup>15</sup>

## Experimental Section

The elements employed were 99.9% K chunks from Baker and 99.998% Tl bars from Johnson-Matthey. These were cleaned with a scalpel before use. The general reaction techniques in welded Ta tubing have been described before.<sup>11,12</sup> Because both reactants and products are exceedingly sensitive to air and moisture, all operations were performed in a  $N_2$ -filled glovebox with a moisture level of less than 0.01 ppm vol.

**Syntheses.** A 1970 phase diagram study by Thümmel and Klemm<sup>17</sup> indicated that KTI is the potassium-richest phase and it melts somewhat incongruently at 268 °C. This is followed by " $K_4Tl_5$ ", now known to be  $K_8Tl_{11}$ ,<sup>15</sup> which melts congruently at 320 °C, and then an incongruently melting  $K_5Tl_8$ . We have put considerable effort into the preparation of single-phase KTI, but so far the highest yield has been ~85%. The following procedures were tested in these efforts: (a) Reactions loaded according to the stoichiometric composition were homogenized at 400 °C for 1 day, slowly cooled to 330 °C (~30 °C above the reported liquidus ~303 °C), and quenched to room temperature in air or in cold water. Such samples were equilibrated for ca. 1 month at 250, 230, 200, or 150 °C and then cooled in air to room temperature. (b) The mixtures from 250 and 230 °C were ground, pressed into pellets, and then annealed at the same temperature as in (a). (c) With the phase diagram as a guide, a reaction was loaded with a 44 atom % Tl composition (just a little bit below the liquidus composition at the peritectic temperature). With the container inclined, this was homogenized at 500 °C for 6 h and at 360 °C for 40 h and then slowly cooled to room temperature at a rate of 2 °C/h. The product in the lower portion of the tube was selected for analysis.

According to Guinier powder patterns, KTI was the major (~85%) phase in (a) and (b) with only  $K_8Tl_{11}$  as a detectable byproduct; traces of K were not seen in the powder pattern, which is usual according to our experience. Procedure c gave a brittle product at the bottom but a soft substance on the surface (excess K metal). The former was found to consist of KTI and an unknown K-richer phase that has not yet been identified. KTI is considered to be a line compound because all powder

\* Abstract published in *Advance ACS Abstracts*, November 1, 1993.

(1) Ames Laboratory is operated for the U.S. Department of Energy by Iowa State University under Contract No. W-7405-Eng-82. This research was supported by the Office of the Basic Energy Sciences, Materials Sciences Division, DOE.

(2) Simon, A. *Angew. Chem., Int. Ed. Engl.* 1988, 27, 160.

(3) Corbett, J. D. In *Modern Perspectives in Inorganic Crystal Chemistry*; Parthé, E., Ed.; NATO ASI Series C; Kluwer Academic Publishers: Dordrecht, The Netherlands, 1992; p 27.

(4) (a) Schaeffer, R.; Johnson, Q.; Smith, G. S. *Inorg. Chem.* 1965, 4, 917. (b) Beaudet, R. A.; Poynter, R. L. *J. Chem. Phys.* 1970, 53, 1899.

(5)  $CaB_6$ : Blum, P.; Bertaut, F. *Acta Crystallogr.* 1954, 7, 81.  $KB_6$ : Naslain, R.; Etoureau, J. C. *R. Acad. Sci. Paris* 1966, 263, 484.  $NaB_6$ : Hagenmuller, P.; Naslain, R. *Compt. Rend.* 1963, 257, 1294.  $LaB_6$ : Korsukova, M. M.; Gurin, V. N.; Lundström, T.; Terenius, L.-E. *J. Less-Common Met.* 1986, 117, 73.

(6) Sevov, S. C.; Corbett, J. D. *Z. Anorg. Allg. Chem.* 1993, 619, 128.

(7) Schiemenz, B.; Hutner, G. *Angew. Chem., Int. Ed. Engl.* 1993, 32, 297.

(8) Corbett, J. D. *Chem. Rev.* 1985, 85, 383.

(9) Greenwood, N. N.; Earnshaw, A. *Chemistry of the Elements*; Pergamon Press: Oxford, U.K., 1984, p 171.

(10) Hiller, W.; Klinkhammer, K.-W.; Uhl, W.; Wagner, J. *Angew. Chem., Int. Ed. Engl.* 1991, 30, 179.

(11) Sevov, S. C.; Corbett, J. D. *Inorg. Chem.* 1991, 30, 4875.

(12) Sevov, S. C.; Corbett, J. D. *J. Solid State Chem.* 1993, 103, 114.

(13) Hansen, D. A.; Smith, J. F. *Acta Crystallogr.* 1967, 22, 836.

(14) Cordier, G.; Müller, V. *Z. Kristallogr.* 1992, 198, 281.

(15) Dong, Z. C.; Corbett, J. D. Unpublished research.

(16) Zintl, E.; Brauer, G. *Z. Phys. Chem.* 1933, 20B, 245.

(17) Thümmel, R.; Klemm, W. *Z. Anorg. Allg. Chem.* 1970, 376, 44.

**Table I.** Selected Data Collection and Refinement Parameters for KTl

space group, $Z$ lattice params, <sup>a</sup> Å	<i>Cmca</i> (No. 64), 24
<i>a</i>	15.329(4)
<i>b</i>	15.069(4)
<i>c</i>	8.137(2)
no. of indep obsd reflns ( $I \geq 3\sigma(I)$ ), variables	462, 33
$\mu$ , cm <sup>-1</sup> (Mo $K\alpha$ )	530.78
transm range	0.77–1.09
residuals: $R$ , $R_w$ <sup>b</sup>	0.037, 0.039

<sup>a</sup> Guinier powder diffraction data;  $\lambda = 1.540562$  Å. <sup>b</sup>  $R = \sum |F_o| - |F_c| / \sum |F_o|$ ;  $R_w = [\sum w(|F_o| - |F_c|)^2 / \sum w(F_o)^2]^{1/2}$ ;  $w = \sigma_F^{-2}$ .

patterns from different compositions gave the same lattice constants within  $3\sigma$ . X-ray powder patterns for samples mounted between pieces of cellophane were obtained with the aid of an Enraf-Nonius Guinier camera, Cu  $K\alpha$  radiation ( $\lambda = 1.54056$  Å), and NBS (NIST) silicon as an internal standard. The resultant cell parameters refined for 46 lines by least-squares are  $a = 15.329(4)$ ,  $b = 15.069(4)$ , and  $c = 8.137(2)$  Å.

**Magnetic Susceptibilities.** Because of our inability to obtain the pure phase of KTl, the susceptibilities of two mixtures of ~85% KTl plus  $K_8Tl_{11}$  (from the reaction annealed at 230 °C) and a sample of X-ray-pure  $K_8Tl_{11}$  were measured. The special container is described elsewhere.<sup>18</sup> Magnetizations were measured at a field of 3 T over 6–300 K on a Quantum Design MPMS SQUID magnetometer.

**Structure Determination.** Shiny, black, platelike crystals were picked up in the glove box and sealed in thin-walled capillaries. Laue, oscillation, and Weissenberg photographs were used to check the singularity of crystals, obtain preliminary lattice parameters, and obtain information for a subsequent space group assignment. A crystallite ca.  $0.15 \times 0.12 \times 0.03$  mm was chosen for data collection, which was carried out on a CAD4 diffractometer. A *C*-centered orthorhombic cell with lattice constants as expected from the film work was obtained after indexing 25 reflections from a random search over  $16 \leq 2\theta \leq 35^\circ$ . Two octants of data were collected with the *C*-centered condition imposed, and these were corrected for Lorentz and polarization effects and for the strong absorption ( $\mu = 531$  cm<sup>-1</sup>) with the average of four  $\psi$ -scans at different  $\theta$  values. Systematic absences in the data indicated only two possible space groups, *Cmca* (No. 64) and *C2ca* (*Aba2*, No. 41). Since the intensity statistics suggested a centrosymmetric space group, *Cmca* was chosen for the first trial and was subsequently proven to be correct on the basis of the successful structure solution and refinement. Some details of the data collection and refinement are listed in Table I.

The structure was successfully solved by direct methods,<sup>19</sup> which gave all atom positions, i.e., two large and three smaller peaks with height ratios of ~4:1 and with reasonable distance around each for Tl and K. A difference Fourier synthesis after their refinement did not reveal any significant peaks. An empirical absorption correction (DIFABS<sup>20</sup>) was applied after the isotropic refinements had converged. A multiplicity refinement of Tl atoms with the K atoms fixed indicated that these sites are fully occupied, with deviations less than  $3\sigma$ . The inverse procedure gave the same answer for the K atoms. The final anisotropic refinement, including a second extinction correction, converged at  $R(F) = 3.7\%$ ,  $R_w = 3.9\%$ , and  $GOF = 1.19$  for 33 variables and 462 independent observed reflections. The largest residual peaks in a final difference Fourier map were  $+1.76$  ( $1.90$  Å from K3) and  $-1.69$  e/Å<sup>3</sup>. Data from a second crystal were later collected without conditions to confirm the *C*-centering, and these refined to a very similar structural result. All calculations were performed using the TEXSAN package.<sup>21</sup>

## Results and Discussion

**Structure Description.** The final positional and isotropic-equivalent thermal parameters are listed in Table II, and the important distances, in Table III. The cell contents shown in Figure 1 describe a quasi-face-centered array of  $Tl_6$  clusters, but two different cluster orientations are related by rotation (or screw) axes, and the structure is only *C*-centered.

(18) Sevov, S. C.; Corbett, J. D. *Inorg. Chem.* **1992**, *31*, 1895.

(19) Sheldrick, G. M. SHELXS-86. Universität Göttingen, Germany, 1986.

(20) Walker, N.; Stuart, D. *Acta Crystallogr.* **1983**, *A39*, 158.

(21) TEXSAN, version 6.0 package; Molecular Structure Corp.: The Woodlands, TX, 1990.

**Table II.** Positional and Isotropic Thermal Parameters and Important Distances for KTl

atom		<i>x</i>	<i>y</i>	<i>z</i>	$B_{eq}$ , <sup>a</sup> Å <sup>2</sup>
Tl1	16g	0.11306(8)	0.39558(6)	0.0689(1)	3.70(5)
Tl2	8f	0	0.5438(1)	0.2193(1)	4.12(7)
K1	8e	1/4	0.2205(6)	1/4	4.6(4)
K2	8d	-0.1774(6)	0	0	4.6(4)
K3	8f	0	0.2002(5)	-0.0751(9)	4.3(4)

$$^a B_{eq} = (8\pi^2/3) \sum_i \sum_j U_{ij} a_i^* a_j^* \bar{a}_i \bar{a}_j.$$

**Table III.** Bond Distances in KTl

Tl1		K1	
Tl1–Tl1	3.466(3)	K1–Tl1	×2 3.680(6)
Tl1–Tl1	3.341(2)	K1–Tl1	×2 3.768(4)
Tl1···Tl1	4.814(2)	K1–K1	×2 4.165(4)
Tl1–Tl2	3.081(2)	K1–K2	×2 4.051(8)
Tl1–Tl2	3.055(2)	K1–K3	×2 4.259(4)
Tl1–K1	3.680(6)		K2
Tl1–K1	3.768(4)	K2–Tl1	×2 3.621(8)
Tl1–K2	3.621(8)	K2–Tl1	×2 3.969(3)
Tl1–K2	3.969(3)	K2–Tl2	×2 3.612(7)
Tl1–K3	3.612(7)	K2–K1	×2 4.051(8)
Tl1–K3	3.671(7)	K2–K3	×2 4.107(9)
	Tl2		K3
Tl2–Tl2	×2 3.081(2)	K3–Tl1	×2 3.612(7)
Tl2–Tl1	×2 3.055(2)	K3–Tl1	×2 3.671(7)
Tl2···Tl2	3.805(3)	K3–Tl2	3.733(8)
Tl2–K2	×2 3.612(7)	K3–Tl2	4.040(8)
Tl2–K3	4.040(8)	K3–Tl2	4.032(8)
Tl2–K3	3.733(8)	K3–K1	×2 4.259(4)
Tl2–K3	4.032(8)	K3–K2	×2 4.107(9)
		K3–K3	×2 4.337(6)

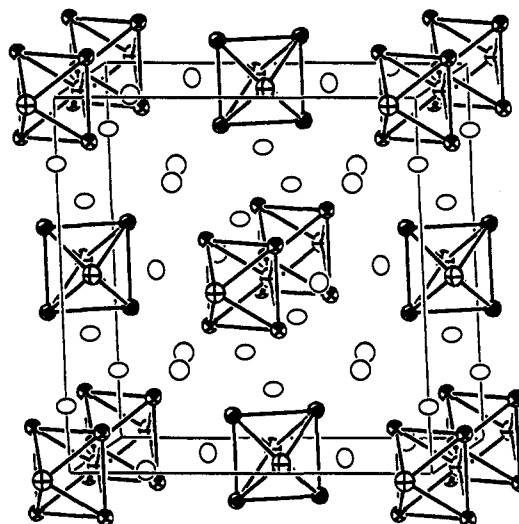


**Figure 1.** Approximate [001] view of the unit cell for KTl showing isolated, approximately octahedral clusters in a pseudo-fcc packing. The 50% probability ellipsoids are shaded for Tl1, crossed for Tl2, and open for K. The *b* axis lies horizontal.

The striking feature of the KTl structure is the presence of the unprecedented, pseudooctahedral  $Tl_6$  clusters illustrated in Figure 2. The cluster has crystallographic  $C_{2h}$  symmetry with the 2-fold axis horizontal through the shorter Tl1–Tl1 separations, while the apical Tl2 atoms lie on the perpendicular mirror plane. A strong axial compression is the principal feature, the trans Tl2–Tl2 distance being only 3.805(3) Å (Pauling bond order<sup>22</sup> = 0.028) versus 4.814(2) Å for the two Tl1–Tl1 diagonals. This means the distances around the “octahedron” fall into two groups, 3.055(2) and 3.081(2) Å for the eight Tl1–Tl2 edges more or less along the compression and 3.341(2) and 3.466(3) Å within the expanded

(22) Pauling, L. *The Nature of the Chemical Bond*, 3rd ed.; Cornell University Press: Ithaca, NY, 1960; p 400.

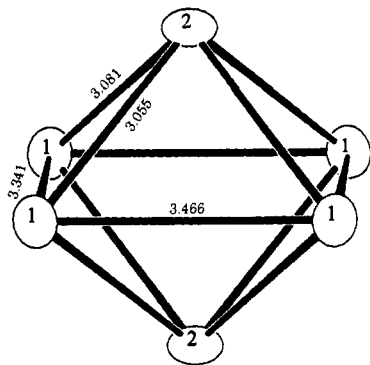


**Figure 2.** The isolated  $\sim D_{2h}$   $Tl_6^{6-}$  cluster anion in KTI, which is strongly compressed along the T12–T12 axis. The actual symmetry is  $C_{2v}$  with the 2-fold axis through the midpoints of the 3.341-Å T11–T11 edges and the perpendicular mirror plane through the T12 atoms, but the deviation from  $D_{2h}$  is very small (40% ellipsoids).

waist. The average of these 12 edges is 3.18 Å, somewhat less than the 3.24-Å edges in  $Tl_4^{8-}$  ( $\sim T_d$ ) and an average of 3.25 Å in  $Tl_{11}^{7-}$ , where there are about equal numbers of 4- and 6-bonded thallium atoms in a pentacapped trigonal prism. The Pauling single-bond metallic diameter is 2.874 Å, and the average edge length corresponds to a bond order of 0.31. The absence of  $D_{2h}$  symmetry and the slight inequalities in the T11–T12 distances originate with a  $0.7^\circ$  tilt of the T12–T12 axis from the normal to the T11 rectangle. This and distortion of the square waist into a rectangle are apparently related to its anisotropic K environment (below). The clusters are well separated, the shortest intercluster distance being 4.756(3) Å (T12–T12).

Earlier work on alkali-metal–indium systems has revealed rather specific arrangements of cations about the main-group metal units,<sup>11,12,18</sup> and the same pertains here. The K–Tl distributions within a range of 3.61–4.04 Å are as follows: Each K1 atom is surrounded by an approximate tetrahedron of T11 atoms in four different clusters, and each T11 has two such exo neighbors. K2 is a  $\mu_2$ -bridging atom on three different clusters, one T11–T11 edge (bisected by the 2-fold axis) and two T11–T12 edges. Each cluster has six such K2 functions, the longest and shortest edges of the cluster being skipped at this point. Finally, each K3 is  $\mu_3$  on the T11–T11–T12 faces that contain the 3.466-Å edges on two different clusters, and it is also exo to T12 in a third. The last is the shortest K3–T12 distance (3.73 Å), and its orientation is presumably responsible for the small deviation of the T12–T12 axis from  $D_{2h}$  symmetry. Figure 3 shows the K distribution about a single cluster in a view normal to the mirror plane so that the K3 disposition can be clearly seen.

**Magnetic Properties.** Only a mixture of KTI and  $K_8Tl_{11}$  was available for measurement (see Experimental Section) for which an 85% KTI and 15%  $K_{0.727}Tl$  ( $=1/11 K_8Tl_{11}$ ) content was estimated on the basis of thallium scattering, powder pattern intensities, reflection multiplicities, and the unit cell contents. Magnetizations of 24- and 27-mg samples were found to be temperature independent ( $\pm 5\%$ ) over the 50–300 K interval, namely  $M = -2.2$  and  $-2.6 \times 10^{-4}$  emu Oe, respectively. These values were apportioned to KTI and  $K_{0.727}Tl$  on the basis of the above estimated composition and an independent measurement on a pure sample of the latter ( $\chi_M = -4.23 \times 10^{-4}$  emu/mol of  $K_8Tl_{11}$  without diamagnetic corrections<sup>15</sup>). The KTI results were thus  $\chi_M = -0.80$  and  $-0.85 \times 10^{-4}$  emu mol<sup>-1</sup> according to  $\chi_M = MF/Hm$  where  $m$ ,  $F$ , and  $H$  are the sample weight, formula weight and field, respectively. Finally, these values were corrected as before<sup>11,12,18</sup> for the diamagnetism of both atomic cores<sup>23</sup> and cluster orbital electrons (Langevin term)<sup>24</sup> ( $-46.5 \times 10^{-6}$  emu mol<sup>-1</sup> total) to give an average  $\chi_M$  value of  $-0.36 \times 10^{-4}$  emu mol<sup>-1</sup> for KTI. The important aspect is the diamagnetism, which

(23) Selwood, P. W. *Magnetochemistry*, 2nd ed.; Interscience Publishers: New York, 1956; p 70.

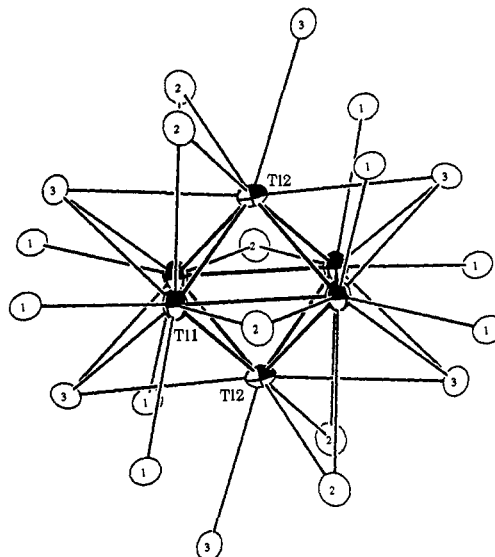


**Figure 3.** Distribution of potassium ion functions about  $Tl_6^{6-}$ . The view is along the 2-fold axis and normal to the mirror plane. All  $K^+$  ions are also coordinated to other, like clusters (see text) (40%). Note the asymmetry in the environment about T12, which is presumably responsible in the small distortion from  $D_{2h}$  symmetry.

eliminates any possibility that significant cluster electrons are delocalized from the cluster into conduction states as they are in  $K_8In_{11}$  and  $K_8Tl_{11}$ .<sup>11,15</sup>

**Bonding.** The thallium sublattice in NaTI, a diamond-like fcc packing, was described as a  $Tl^-$  lattice in a classical Zintl-Klemm picture,<sup>16,25</sup> with good merit according to recent studies.<sup>26</sup> Of course, if we consider only the topological structure, every Tl atom in the present KTI is also 4-bonded (4b) to other Tl atoms, viz.,  $4b-Tl^-$ , but not in the prototypical structure. In fact, the second description contradicts more conventional (Wade's rule<sup>27</sup>)-wisdom that would predict a  $Tl^{(8/6)-}$  oxidation state for an octahedron with  $2n + 2 = 14$ , not  $2n$ , skeletal electrons because of the addition of a seventh radial bonding orbital. The distortion we observe must correlate with the apparent hypoelectronic character of  $Tl_6^{6-}$ . This conclusion is supported fairly well by extended Hückel calculations on the cluster. However, optimized and tested orbital parameters for thallium in this (or any other) type of system have not been published,<sup>28</sup> so we performed calculations with several sets of parameters.<sup>29</sup> The result of the observed compression (and equatorial expansion) are actually rather easy to anticipate intuitively.

As shown in Figure 4 for one set of SCF parameters,<sup>30</sup> the classical octahedral  $Tl_6$  with the same average distance gives six mainly s and seven mainly p bonding orbitals with the following energies (eV):  $a_{1g}$ , -15.47;  $t_{1u}$ , -12.14;  $e_g$ , -9.17;  $t_{2g}$ , -7.20;  $t_{1u}$ , -6.16;  $a_{1g}$ , -5.94 eV below a  $t_{2u}$  LUMO at -4.66 eV (not shown). The tetragonally compressed ( $D_{4h}$ ) result with average distances of the observed cluster appropriately splits the higher  $t_{1u}$  into  $e_u$ , -6.31 eV, and  $a_{2u}$ , -5.56 eV, with the largely unaffected  $a_{1g}$  intervening at -5.91 eV. This produces a plausible gap (0.35 eV)

(24) Ashcroft, N. W.; Mermin, D. N. *Solid State Physics*; Holt, Rinehart and Winston: Philadelphia, PA, 1976; p 649.

(25) Klemm, W.; Busmann, E. *Z. Anorg. Allg. Chem.* **1963**, *319*, 297.

(26) Schmidt, P. C. *Struct. Bonding* **1987**, *65*, 91.

(27) Wade, K. *Adv. Inorg. Chem. Radiochem.* **1976**, *18*, 1.

(28) Janiak, C.; Hoffmann, R. *J. Am. Chem. Soc.* **1990**, *112*, 5924.

(29) Two sets employed  $H_{ss} = -11.60$ ,  $H_{pp} = -5.80$  eV with orbital exponents ( $\xi$ ) either used before (2.30, 1.60)<sup>28</sup> or taken from SCF calculations (2.14, 2.04).<sup>30</sup> Other more recent SCF parameters (-12.80, -5.10 eV;  $\xi = 2.52$ , 1.77)<sup>31</sup> were also examined, as were the set recently applied to thallium superconductors (-16.2, -9.0 eV;  $\xi = 2.37$ , 1.97).<sup>32</sup>

(30) Clementi, E.; Raimondi, C. L.; Reinhardt, W. P. *J. Chem. Phys.* **1967**, *47*, 1300.

(31) Clementi, E.; Roetti, C. *At. Nucl. Data Tables* **1974**, *14*, 177.

(32) Kang, D. B.; Jung, D.; Whangbo, M.-H. *Inorg. Chem.* **1990**, *29*, 257.

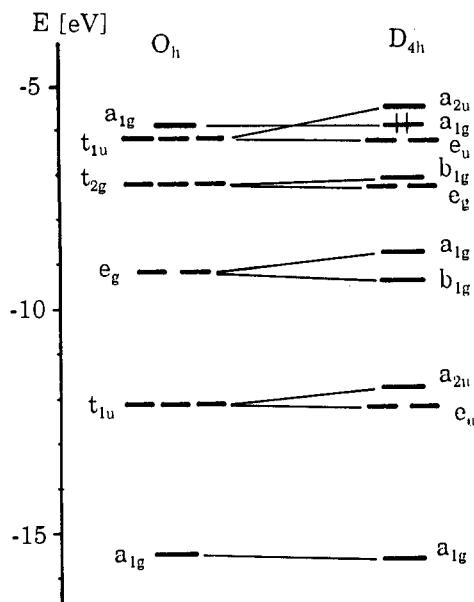
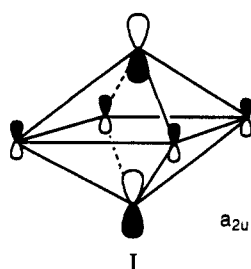


**Figure 4.** Extended Hückel results for the ideal octahedral  $Tl_6$  ( $O_h$ ) and for the tetragonally compressed example ( $D_{4h}$ ) as calculated with one set of SCF parameters for Tl.<sup>30</sup>

above the last for 12 electron pairs (s and p) at the point where the net orbital overlap populations also change from +0.49 ( $a_{1g}$ ) to -0.10 ( $a_{2u}$ ). Going to the observed  $C_{2v}$  symmetry hardly changes these at all. More tightly bound levels and a similarly small p orbital<sup>32</sup> produce a comparable result with a 0.79-eV gap. On the other hand, use of a different SCF set<sup>31</sup> with a greater s-p separation and a larger p orbital puts the  $a_{1g}$  nearly 2.0 eV above  $e_u$ , with the intervening  $a_{2u}$  and a  $b_{2u}$  LUMO (from  $t_{2u}$ ) separated by 0.55 eV. This last result seems rather implausible; the presumed  $a_{2u}$  HOMO is antibonding, while the higher  $a_{1g}$  remains moderately bonding. The results are not very convincing because of the lack of a proven parameter set. Calculations with only p orbitals give a result consistent with first calculation, while the orbital values recently employed for Tl(I) calculations<sup>28</sup> do not afford a significant gap for 24 total electrons.

There is not much point in pursuing the question further; we are not only using one-electron Hückel approximations but are also ignoring serious relativistic effects,<sup>33</sup> including a significant difference between the  $6p_{1/2}$  and  $6p_{3/2}$  orbitals, which is  $\sim 1.0$  eV in neutral Tl.<sup>31</sup> But the principle is clear enough; compression will certainly drive the  $a_{2u}$  orbital higher, presumably enough to give us the observed  $2n$  configuration. Although the  $a_{2u}$  orbital I, which follows  $p_z$ , is  $\sigma$  bonding between the axial atoms and the



square, the compression leads to an increased  $\pi^*$  effect for the same atom pairs, a loss of  $\pi$  within the enlarging waist, and a strongly antibonding T12-T12 interaction along the compression axis. A Jahn-Teller approach to the problem starting with the 24-electron octahedron predicts the same thing.

Compression of a classical cluster as a means to reduce the electron requirements is not new in concept or in recent practice. Thallium's congener indium has already demonstrated this process twice. Compression of the pentacapped trigonal prism ( $D_{3h}$ ) so as to expand the triangular prism faces normal to the principal axis and to bring the different types of capping atoms into bonding interactions removes one orbital from the bonding set, thus accounting for the observed  $In_{11}^{7-}$ ,  $Tl_{11}^{7-}$ , and  $In_{10}Hg^{8-}$ .<sup>11,15,35</sup> The same thing occurs for the bicapped antiprismatic  $In_{10}Zn^{10-}$  and  $Tl_{10}Zn^{10-}$  centered by zinc.<sup>15,36</sup> Compression of the conventional  $D_{4d}$  figure (which serves to bring all In or Tl vertices to about the same distance from Zn) opens up the capped square faces and squashes the antiprism, which in turn produces reduced bonding and increased antibonding effects in the critical  $a_1$  orbital. The magnitude of the distortion necessary, and the rate at which the one orbital is raised is less with a capped square than with a capped triangle.<sup>37</sup>

Although we have not been able to synthesize a pure KTI phase for conductivity studies, the clear diamagnetism of the phase strongly encourages a closed-shell, valence compound interpretation. Similarly corrected diamagnetic characteristics,  $-3.0$  to  $-5.0 \times 10^{-4}$  emu mol<sup>-1</sup>, and clear electron localization are encountered for the apparently closed-shell cluster phases  $K_8-In_{10}Zn$ ,  $K_8-In_{10}Hg$ , and  $K_{10}In_{10}Z$  ( $Z = Ni, Pd, Pt$ ), even though the conductivities of the first two are of the nature of semimetals or poor metals.<sup>35,36,38</sup> A rather striking parallel exists between strong covalent bonding characteristics of thallium and indium in anionic states that are so evident in their solid alkali-metal compounds and the conduction properties of the same liquid alloy systems. The latter show strong dependencies of melt conductivity on composition, with distinct minima near 50 atom % for either Tl or In when these are paired with K, Rb, or Cs. (The minima progressively diminish and shift toward alkali-metal-richer compositions with Na and Li.) The resistivities reach 400-900  $\mu\Omega$  cm at or near 1:1 with a parallel dip in  $d\rho/dT$  to quite negative values, i.e., corresponding to activated (semiconduction-like) processes.<sup>39,40</sup> The presence of classical cluster species like  $Pb_4^{4-}$  is fairly well accepted in analogous lead melts,<sup>41</sup> and these clusters are, of course, well-known in solid phases.<sup>42</sup>

The present  $Tl_6^{6-}$  ion represents the first example of an isolated thallium cluster with a suitable 1:1 charge:atom ratio (or phase composition), and the description of another,  $Tl_9^{9-}$ , will be forthcoming.<sup>15</sup> Strangely enough, there are none in the better known, condensed binary indium systems, only  $In_{11}^{7-}$  and  $In_4^{8-}$ , and no isolated homoatomic gallium cluster of any sort has been reported. However, the options in crystalline solids are restricted considerably by the needs for long-range order, efficient packing, and, frequently, precise valence conditions, or nearly so. Thus, rather elegant network structures of interbonded indium clusters of a considerable variety may be formed, and subtle changes in cation sizes and proportions can influence the network obtained considerably.<sup>6,12,18,43</sup> The liquid state can afford a considerable simplicity in this respect, but a larger variety of species may be present within a single system as well. Some remarkable specificities in these melts are implied.<sup>44</sup> Nonetheless, thallium does seem to provide significantly more examples of isolated clusters in solid binary phases, as we shall further document.<sup>15</sup>

(35) Sevov, S. C.; Corbett, J. D. *J. Alloys Comp.*, in press.

(36) Sevov, S. C.; Corbett, J. D. *Inorg. Chem.* **1993**, *32*, 1059.

(37) An alternative bicapped tetrahedral, or uncapped trigonal bipyramidal, geometry with 12 skeletal electrons that is consistent with the counting rules is known in the ligated  $Os_6(CO)_{18}$  [Mason, R.; Thomas, K. M.; Mingos, D. M. P. *J. Am. Chem. Soc.* **1973**, *95*, 3802. Wade, K. In *Transition Metal Clusters*; Johnson, B. F. G., Ed.; Wiley: Chichester, U.K., 1980; p 233].

(38) Sevov, S. C.; Corbett, J. D. *J. Am. Chem. Soc.* **1993**, *115*, 9089.

(39) Itami, T.; Izumi, K.; Iwaoaka, N. *J. Non-Cryst. Solids* **1993**, *156-158*, 285.

(40) Xu, R.; van der Lugt, W. *J. Non-Cryst. Solids* **1993**, *156-158*, 289.

(41) van der Lugt, W. *Phys. Scr.* **1991**, *T39*, 372.

(42) Hewaldy, I. F.; Busmann, E.; Klemm, W. *Z. Anorg. Allg. Chem.* **1964**, *328*, 283.

(43) Sevov, S. C.; Corbett, J. D. *Inorg. Chem.* **1993**, *32*, 1612.

(33) Pyykkö, P. *Chem. Rev.* **1988**, *88*, 563.

(34) Desclaux, J. P. *At. Nucl. Data Tables* **1973**, *12*, 311.

In the present case, the KTI cluster phase as an alternative to the classical "stuffed" (or double interpenetrating) diamond structure known for prototypical NaTI must result from the equal-size requirement for the two networks that has long been recognized for the latter.<sup>16</sup> In another case, the Na-In system, the inclusion of small amounts of cluster-forming elements like Ni leads to the formation of remarkable fullerene-like condensed cages of In, more evidence of the strong covalent bonding tendencies of anionic Ga, In, and Tl.

**Acknowledgment.** J. D. Martin and G. J. Miller provided advice regarding the calculations, and J. Ostenson measured the magnetic susceptibility data.

**Supplementary Material Available:** Tables of data collection and refinement details and anisotropic displacement parameters for the atoms in KTI (2 pages). Ordering information is given on any current masthead page.

---

(44) van de Lugt, W. Private communication, 1993.  
(45) Sevov, S. C.; Corbett, J. D. *Science*, in press.